

SOME ASPECTS OF PHYSICAL METALLURGY OF MICROALLOYED STEELS

Nenad Radović^{1}, Goran Vukićević², Dragomir Glišić¹, Stefan Dikić^{1*}*

¹ *Department of Metallurgical Engineering, Faculty of Technology and Metallurgy,
University of Belgrade, Serbia*

² *HBIS GROUP Iron and Steel d.o.o. Serbia, Hot Strip Mill, Smederevo, Serbia*

Received 31.12.2019

Accepted 06.01.2020

Abstract

Some aspects of deformation, precipitation, and recrystallization behavior in medium carbon V-microalloyed and low carbon Nb/Ti-microalloyed steels are presented in the paper. Changes in microstructure are explained together with methods of quantification. The temperature of No-recrystallization (T_{nr}) is defined as a milestone to show the onset of retardation of recrystallization while the apparent activation energy for hot working shows the extent of this retardation. In the case of high cooling rates, this method is not sufficiently sensitive and T_{rl} (recrystallization limit temperature) and T_{rs} (recrystallization stop temperature) must be evaluated from softening data. Paper presented the possibility to estimate T_{nr} temperature on six stands finishing train at Hot Strip Mill in HBIS Iron and Steel Serbia, Smederevo as well as the activation energy for static recrystallization, QSRX, derived from T_{nr} temperatures.

Keywords: microalloyed steels; deformation; recrystallization; precipitation; Boratto test.

Introduction of micro-alloyed steels to industrial practice

Microalloyed steels are commonly considered to be steels in which small addition of alloying (particularly Nb, V and/or Ti up to 0.15% in total) elements lead to intensive grain refinement and/or precipitation of stable carbides, nitrides or carbonitrides [1-6].

Grain refinement in MA steels is provided by retardation of recrystallization of austenite during thermomechanical processing via the presence of MA elements in solid solution or precipitation of their carbides, nitrides or carbonitrides.

Another beneficial behavior is related to the formation of nitrides/carbonitrides that act as preferential places for nucleation of phases with improved toughness [7, 8].

*Corresponding author: Nenad Radović, nenrad@tmf.bg.ac.rs

The main reasons for the application of MA steels were significant increase in strength together with good toughness, cheaper production via thermomechanical treatment in comparison to fine grain steels and a demand for steels with improved weldability for pressure vessels and pipelines, in which increase of strength by heavier alloying and carbon content limited weldability [9-12].

Thermomechanical processing of MA steels

Single-pass testing. Temperature and strain rate dependence of stress during hot deformation can be described using equation (1), initially developed for creep [13] and later suggested for a wide range of stresses in hot deformation [14-20].

$$Z = \dot{\varepsilon} \cdot \exp\left(\frac{Q_{HW}}{RT}\right) = A_3 \cdot [\sinh(\alpha\sigma)]^{n'} \quad 1$$

Where A_3 , n' and α - constants

Z – Zener-Hollomon parameter – temperature compensated strain rate.

$\dot{\varepsilon}$ – strain rate, s^{-1}

T – temperature, K,

R – universal gas constant, 8,315J/mol·K,

Q_{HW} – apparent activation energy for hot working, J/mol.

σ - stress at any predefined strain or peak stress during continuous isothermal test

Set of stress-strain curves for one medium carbon microalloyed steel containing 0.31% C, 1.55% Mn, 0.13% V, and 0.012 %N are shown in Figure 1, details given in the literature [17].

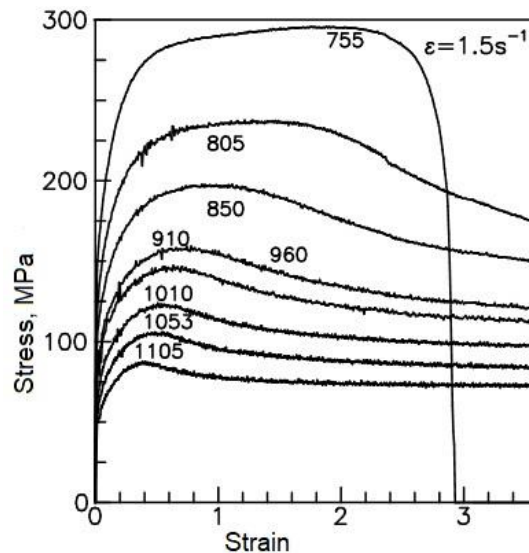


Fig. 1. Stress strain curves of V-steel (designated temperatures at $\varepsilon=\varepsilon_p$, °C) [17].

Using peak stress and stress at 0.35, the apparent activation energy for hot working, Q_{HW} , was calculated based on equation (1). The results are shown in Figure 2 [17].

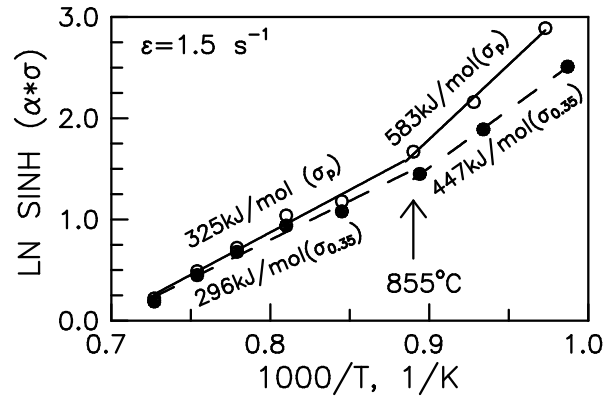


Fig. 2. Stress-temperature dependence obtained at strain rate $\dot{\epsilon} = 1,5 \text{ s}^{-1}$; calculated values for Q_{HW} are given on picture [17].

The apparent activation energy for hot working, Q_{HW} , depends both on strain and temperature. Figure 2 clearly shows two different linear segments for lower and higher temperatures. Therefore, it was possible to estimate Q_{HW}^L and Q_{HW}^U for the low-temperature region, Q_{HW}^L , and Q_{HW}^U for the upper part (higher temperatures), Q_{HW}^U . The temperature at which two slopes intercepts is 855°C . This behavior was firstly reported for high carbon-high alloyed high-speed tool steels [21, 22]. It was assumed that at certain temperature dynamic recrystallization is suppressed by precipitation. These steels and MA steels are both susceptible to a precipitation reaction during deformation at high temperatures. Therefore, similar behavior in tested steel is attributed to precipitation at lower temperatures, i.e., inhibition of dynamic recrystallization leads to much higher values for Q_{HW}^L . These results also suggest that for modeling of deformation behavior both Q_{HW}^L and Q_{HW}^U should be used for lower and higher temperatures respectively.

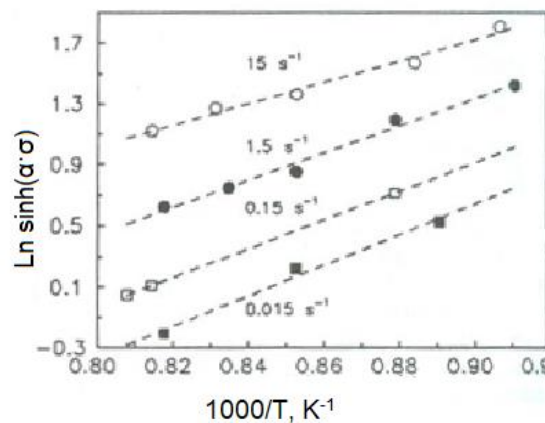


Fig. 3. Temperature dependence of peak strain using eq (1) [19].

The apparent activation energy for hot working, Q_{HW} , also depends on the strain rate. Figure 3 shows the peak stress dependence of temperature. Tested Nb/Ti steel (details given in [19]) containing 0.08% C, 1% Mn, 0.035% Nb, and 0.017% Ti exhibits different slopes depending on strain rate per pass. For samples deformed at strain rates $0.015s^{-1}$, $0.15s^{-1}$, $1.5s^{-1}$, $15s^{-1}$, Q_{HW} have values of 453 kJ/mol, 423 kJ/mol, 404 kJ/mol, and 318 kJ/mol. The last value, similar to the value of activation energy for self-diffusion in Fe [23], was estimated in test in which the whole deformation was finished in a fraction of second, implying that no precipitation took place.

Multi-pass testing. Single-pass hot working is present only in extrusion or sometime in forging, i.e., in all other cases, hot working is multipass technology. Considering multipass deformation at high temperatures, the occurrence of different features must be taken into account, both during deformation pass and interpass interval.

Process parameters that define deformation are previous grain size, strain rate, strain per pass and pass temperature. During deformation, two opposite trends can be expected: (i) increase in dislocation density due to deformation and (ii) decrease of dislocation density due to restoration processes. Therefore, deformation hardening, or dynamic recovery or dynamic recrystallization or dynamic precipitation can occur. During interpass interval, static recovery or static recrystallization or metadynamic recrystallization or static precipitation, depending on interval temperature and interpass time may occur [1, 3, 13, 14, 23].

The microstructure of MA steels after Thermomechanical processing is characterized by small and homogenous ferrite (α) grains. Some minor amount of Fe_3C is usually present, together with very fine dispersed carbonitride particles. After the final pass during finishing hot rolling, nucleation of α grains during cooling below Ar_3 temperature occurs at many defects. In order to keep these defects (grain and subgrain boundaries, dislocations, deformation bands and twins) static recrystallization must be suppressed. The mechanism of recrystallization is the formation of nondeformed nuclei and its further growth. Recrystallization can be suppressed/postponed due to the presence of alloying elements in solid solution (continuous finish rolling - short interpass times) or precipitation during interpass times (reverse rolling - long interpass times). In both cases, grain and subgrain boundary mobility are decreased [1, 3, 5, 6].

The thermomechanical processing of MA steels is a dominant production route for steels with both high YS and improved toughness. Schematic illustration of TMCP of microalloyed steels is given in Figure 4 and includes several possible technologies [1, 5, 6]:

- [1] Recrystallization Control Rolling (RCR). Complete rolling (both roughing and finish rolling) are in the region of full static recrystallization between passes (above T_{nr} - temperature). Since total deformation is in recrystallization temperature range, prior γ relatively coarse grains (Fig.4, sketch a) after deformation transforms into microstructure consisting of smaller recrystallized α grains (Fig.4, sketch b);
- [2] Conventional Control Rolling (CCR). The first stage of rolling (roughing) is performed in the temperature range in which full static recrystallization between passes takes place (above T_{nr}), and finish rolling takes place on lower temperatures, i.e. in the temperature range in which static recrystallization is suppressed (between T_{nr} and Ar_3). Recrystallization can be suppressed either by

precipitation (reverse rolling - long interpass times) or presence of alloying elements in solid solution (continuous finish rolling - short interpass times, absence of precipitation) [5,6]. After deformation is finished, the microstructure consists of elongated γ grains with deformation bands and twins within (Fig.4, sketch c). They serve as ferrite grains nucleation sites during cooling after the final pass. The resulting microstructure has very fine grains (Fig.4, sketch c'). This technology is in the highest use in industry, particularly for hot strips for pipelines with width up to 18mm, depending on the coiler.

- [3] Two-Phase Rolling. This technology is a modification of CCR technology, i.e. several passes are executed in the two-phase region. Consequently, after rolling microstructure consists of both deformed austenite and ferrite grains (Fig.4, sketch d). After cooling, austenite grains will transform into small ferrite grains, while deformed ferrite grains will recrystallize and become finer (Fig.4, sketch d'). In some cases, the limitation of this technology is high resistance to deformation.
- [4] Dynamic Recrystallization Control Rolling (DRCR). The main goal of this modification of CCR technology is to provide dynamic recrystallization. Therefore, the total strain on finishing rolling of deformation from pass to pass must lead to exceeding a critical strain for dynamic recrystallization. Overall strain in finish rolling is higher than in CCR and it is accumulated from pass to pass. The effect of grain refinement is the strongest in this case;
- [5] Conventional Control Rolling + Accelerated Cooling (CCR+AC). Generally, accelerated cooling increases undercooling providing higher nucleation rate and finer final structure. On the other hand, if the cooling rate is high enough, bainitic ferrite can be produced with or without ferrite. This bainitic ferrite will increase strength with remaining excellent toughness.

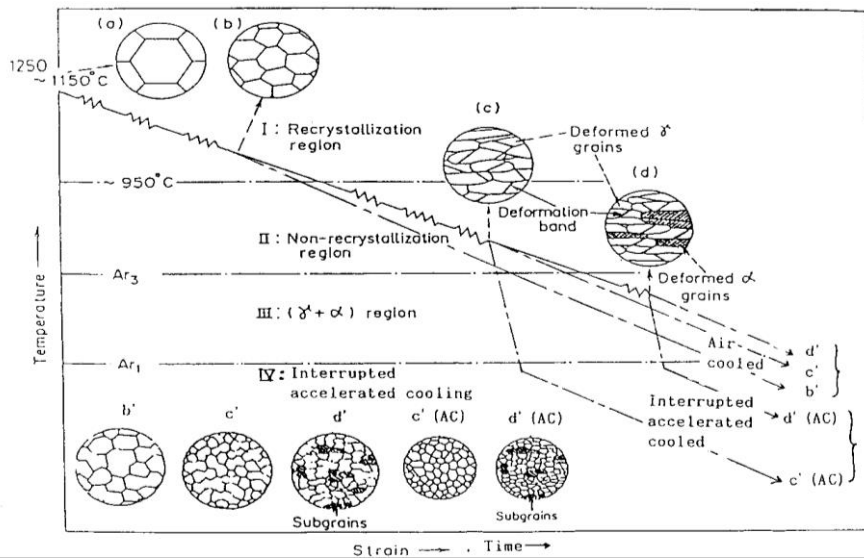


Fig. 4. Thermomechanical rolling of microalloyed steels [5].

Critical temperatures for hot rolling of microalloyed steels. It is clear that the determination of temperature that divides temperature regions for rough rolling and finish rolling is of the highest importance. In that respect, *F. Boratto et al.* [24] established anisothermal multipass test, consisting of 20 passes with constant strain and strain rate per pass. The first pass is performed at high temperatures (usually above 1100 °C), with a decrease of temperature for each subsequent pass. For each pass, mean flow stress was calculated as the surface below the stress-strain curve and plotted vs. reverse pass temperature, eq. (2) [17-19, 24-27].

$$MFS = \frac{1}{\varepsilon_b - \varepsilon_a} \int_{\varepsilon_a}^{\varepsilon_b} \sigma d\varepsilon \quad 2$$

Where: σ – stress, MPa, and ε -strain.

This dependence shows two different slopes, for a high-temperature region in which full recrystallization takes place and for a low-temperature region in which recrystallization is not completed/absent. Intersection of two slopes defines T_{nr} temperature (non-recrystallization temperature) [17-19,24-27]. It is assumed that finish rolling should be below this specific temperature. Also, since the suppression of recrystallization can be achieved via precipitation and/or presence of alloying elements in solid solution, *Dutta and Sellars* suggested temperature at which is the onset of partial static recrystallization, T_{rl} , and temperature at which static recrystallization is completely suppressed, T_{rs} [28]. This approach is based on interpass softening, eq (3), a method introduced by *Liu and Akben* [29] and quantified by *Drobnjak et al.* [17-19].

$$FS = \frac{\sigma_m^i - \sigma_y^{i+1} \cdot \frac{\sigma_0^i}{\sigma_0^{i+1}}}{\sigma_m^i - \sigma_0^i} \cdot 100, \% \quad 3$$

Where,

σ_0 and σ_m are yield stress and maximum pass stress
i and i+1 are previous and subsequent deformation pass

In order to establish the influence of interpass time on T_{nr} temperature, a series of tests with interpass times between 1.8 and 100 seconds were performed on Nb/Ti steel (see details in the literature [17-19]). Stress-strain curves, MFS vs. 1/T and FS vs. 1/T dependences are shown in figures 5 - 7.

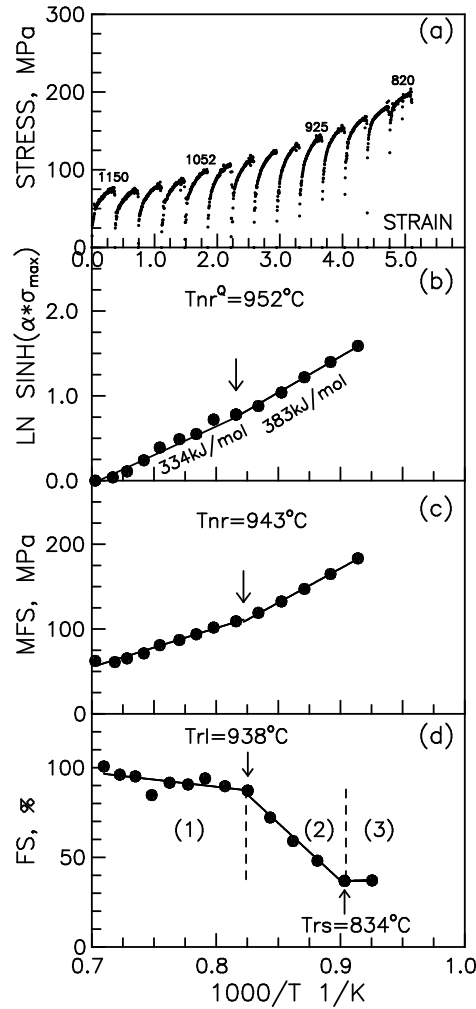


Fig. 5. Nb-steel deformed in torsion using interpass time of 30 s, pass strains of 0.35, strain rate of $1.5s^{-1}$ and cooling rate of $0.84\text{ }^{\circ}C/s$; (a) Stress-strain curves; (b) Dependence of pass-to-pass maximum stress, σ_{max} on pass temperature using Eq.(1); (c) Dependence of mean flow stress (MFS) on pass temperature; (d) Dependence of fractional softening (FS) on mean interpass temperature[19].

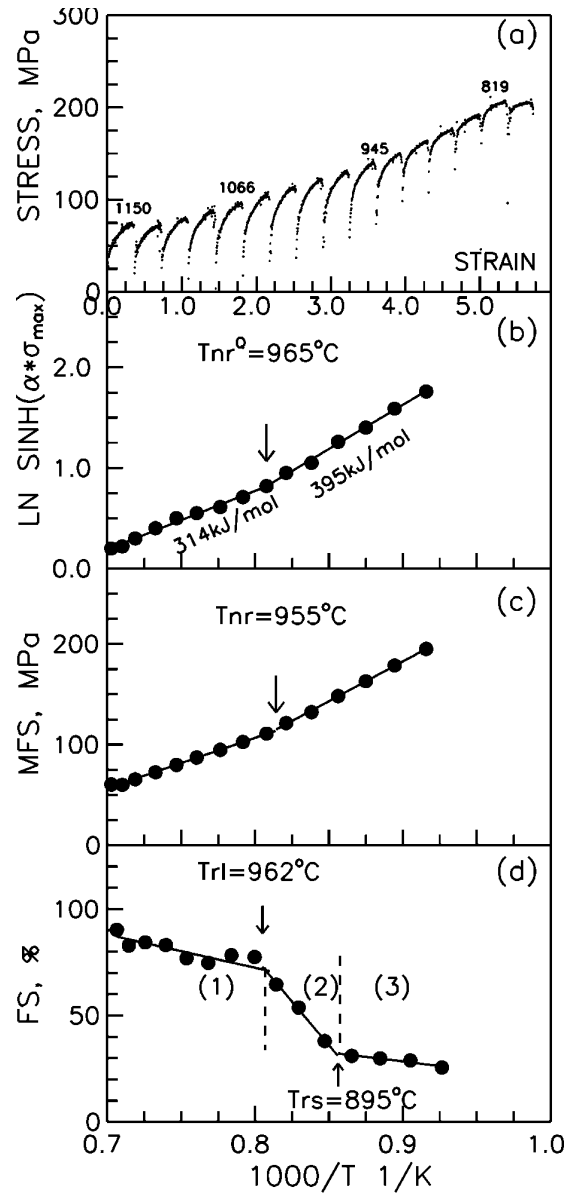


Fig. 6. Nb-steel deformed in torsion with interpass time of 5s, pass strain of 0.35, strain rate of $1.5s^{-1}$ and cooling rate of 5°C/s ; (a) Stress-strain curves; (b) Dependence of pass-to-pass maximum stress, σ_{max} , on deformation temperature; (c) Dependence of mean flow stress (MFS) on deformation temperature; (d) Dependence of fractional softening (FS) on mean interpass temperature [19].

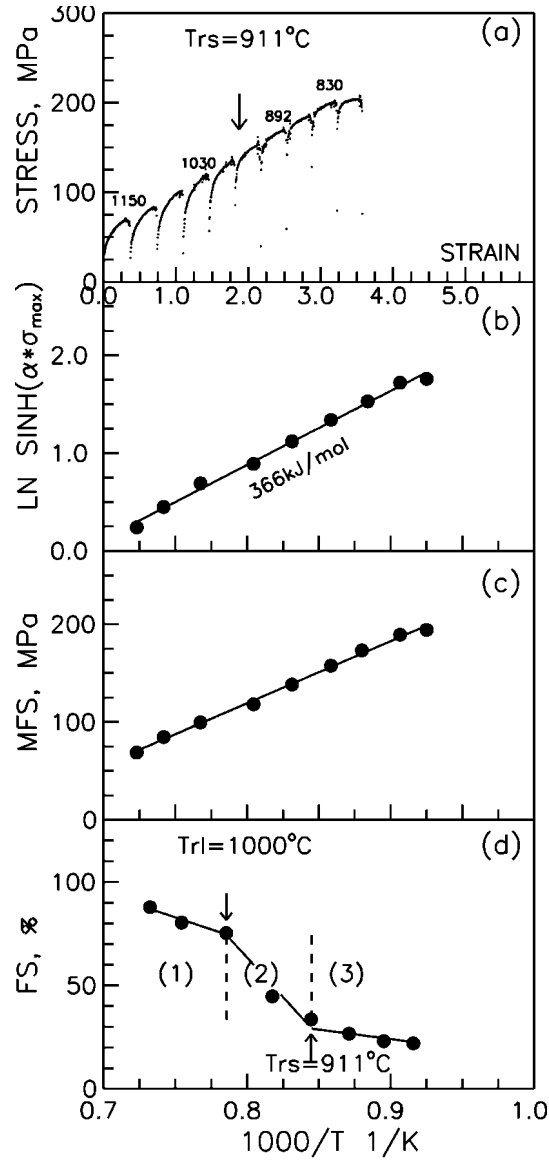


Fig. 7. Nb-steel deformed in torsion with interpass time of 2.7s, pass strain of 0.35, strain rate of 1.5 s^{-1} and cooling rate of 14.1 °C/s ; (a) Stress-strain curves; (b) Dependence of pass-to-pass maximum stress, σ_{max} , on deformation temperature; (c) Dependence of mean flow stress (MFS) on deformation temperature; (d) Dependence of fractional softening (FS) on mean interpass temperature [19].

Based on figures 5a and 6a T_{nr} can be evaluated based on the shape of the stress-strain curve, i.e. in the temperature range above T_{nr} , all individual stress-strain curves exhibit high strain hardening rate (passes 1-6, fig 5a and passes 1-9, fig 6a). On the other hand, the low strain hardening rate is dominant in the temperature region below T_{nr} . More accurately, T_{nr} was estimated based on MFS vs. $1/T$ plot, figures 5c and 6c. In the high-temperature region, full recrystallization takes place between passes, while below T_{nr} recrystallization is suppressed. This implicates different microstructures, and need to estimate apparent activation energy for hot working, Q_{HW} , both over and below T_{nr} , as shown in Figures 5b and 6b. The T_{nr} temperature estimated at the intersection of two slopes is in good agreement with value on fig 5b and 6b. From fig. 5d and 6d are estimated T_{rl} and T_{rs} temperatures, based on the change of slope of fraction softening, eq(3)[17-19].

Results shown in Figure 7 are obtained for interpass time of 2.7 seconds but under an increased cooling rate. The set of stress-strain curves, Figure 7a shows that not a single pass exhibits a high strain hardening rate, which is characteristic of the recrystallized structure. This fact is confirmed on Figures 7b and 7c on which is only one slope present, indicating partial recrystallization over the whole range of temperatures. On the other hand, T_{rl} and T_{rs} were determined, showing that both T_{rl} and T_{rs} values are relatively high. This result also indicates that methodology based on MFS vs. $1/T$ is not sensitive enough for high cooling rates [17-19].

Interpass time dependence of apparent activation energy for hot working, Q_{HW} , for V and Nb/Ti steels are shown in Figures 8 and 9, respectively.

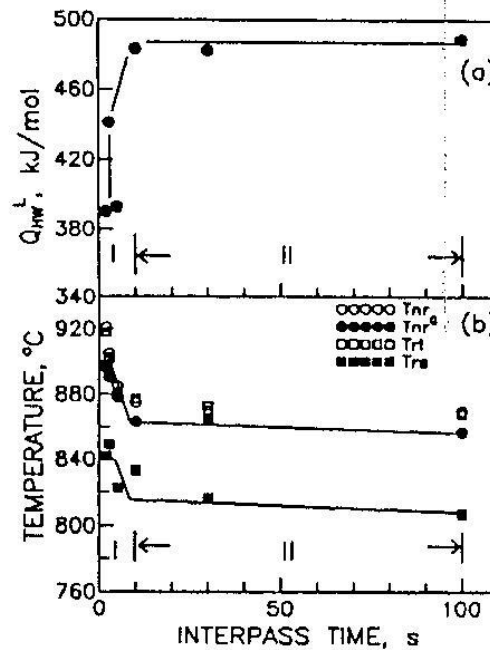


Fig. 8. Interpass time dependence of apparent activation energy for hot working, Q_{HW} , for V steel [17].

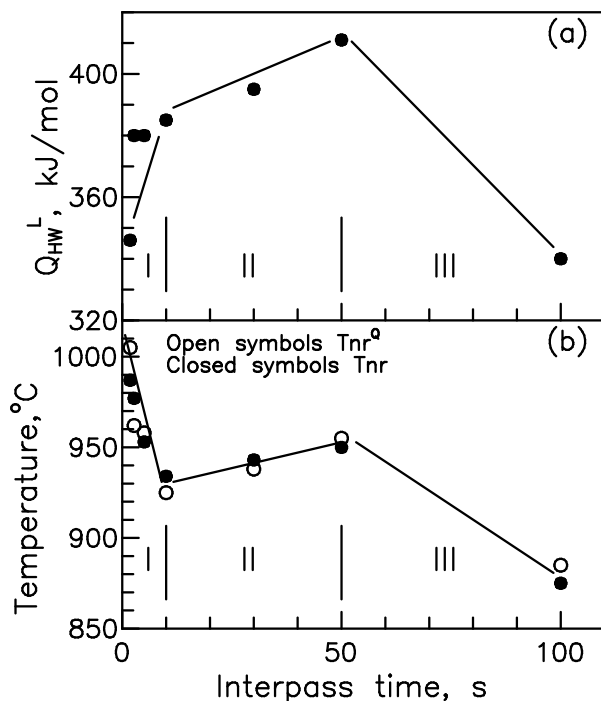


Fig. 9. Interpass time dependence of apparent activation energy for hot working, Q_{HW} , for Nb/Ti steel [19].

Dependence for V-steel can be divided into two regions. In the first one, below 10 seconds, Q_{HW} , and T_{nr} exhibit opposite trends, i.e. Q_{HW} , increases while T_{nr} decreases. It is assumed that, due to short interpass times, no precipitation takes place, implying that solution drag is responsible for the suppression of recrystallization. For interpass times longer than 10 seconds, both Q_{HW} and T_{nr} show similar behavior. After precipitation starts and controls recrystallization, VN particles are produced during the whole range, providing almost constant values of both parameters [17, 18].

In the case of Nb/Ti steel, three regions can be observed. In short interval times (below 10 seconds), as in V steels, Q_{HW} , increases while T_{nr} decreases, also due to solute drag control of recrystallization. In the second region (10 to 50 seconds), value increases suggesting that precipitation is more effectively suppress recrystallization in comparison to solute drag. The values of Q_{HW}^L obtained in this region are in good agreement with values from figure 3. At long interpass times, the third region between 50 and 100 seconds, both Q_{HW} and T_{nr} decreases. This behavior is related to the start of precipitation of NbCN particles in the second region and their coarsening in the third region [18, 19].

This behavior can be described by the CCT diagram shown in Figure 10 [19]. For a wide range of interpass times, each cooling rate is drawn and each deformation step is designated with small full circle, while a large closed circle denotes the position of T_{nr} (T_{rl}) and T_{rs} temperatures. Large open symbols and precipitation start temperature, T_{ps} (dashed/dotted line) are taken from the reference [26]. It can be seen that at short interval times, T_{nr} is higher than expected precipitation start temperature, T_{ps} , i.e., some other mechanism must be responsible for the suppression of recrystallization. When time is increased, precipitation starts and immediately suppresses recrystallization in a subsequent pass. Figure 10 reveals the relationship between deformation, precipitation and recrystallization. Strain per pass in these tests was $\epsilon=0.35$, which is average pass strain on finish rolling at Hot Strip Mill HBIS Iron and Steel Serbia in Smederevo.

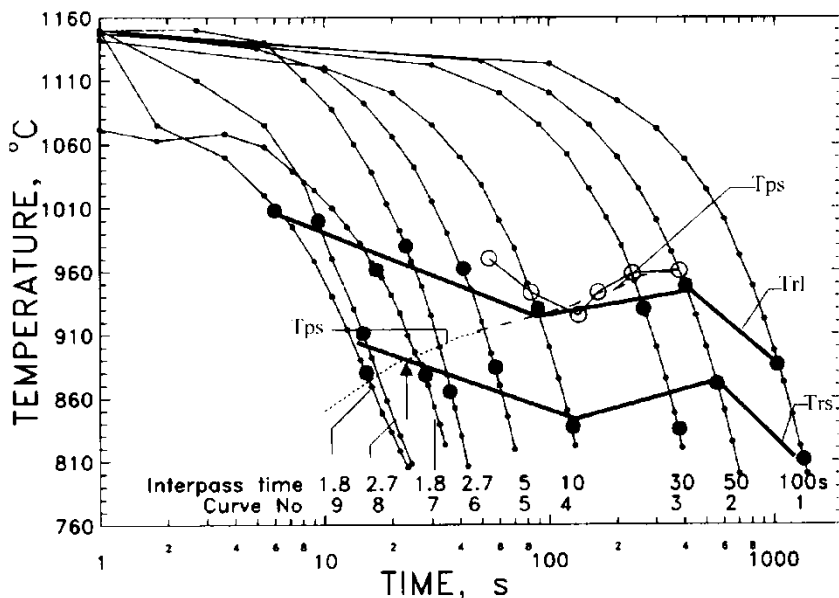


Fig. 10. Interpass time dependence of T_{nr} temperature and precipitation start time T_{ps} . (small closed symbols – deformation steps; large closed symbols – T_{nr} temperatures obtained in this work; large open symbols – T_{nr} temperatures reported in [26]; dashed line – precipitation start time for the same steel [26]) [19].

Industrial-scale. Hot rolling can be performed on reversing mill or on finish multi-strand train. They are characterized by long interpass times, up to 30 s, and very short interpass times, between 1.7-5 s, respectively. The latter in Hot Strip Mill Smederevo includes a six-stand finish train. As mentioned earlier, finish rolling below T_{nr} temperature causes grain flattening, which, in turn, promotes extensive ferrite nucleation, leading to uniform grain refined microstructure, providing good mechanical properties.

Sims's approach and temperature model for finish rolling were used in order to convert roll stand data to mean flow stress (MFS), and calculate temperature (T), respectively. Mean flow stress (MFS) was calculated using equation (4) [30]:

$$MFS = \frac{F}{\frac{2}{\sqrt{3}} \cdot b \cdot \sqrt{R \cdot \Delta h} \cdot Q} \cdot 9810, MPa$$

4

where:

F – rolling force, kN

b – strip width, mm

R – radii of working rolls, mm

$\Delta h = h_1 - h_2$ – absolute reduction

Q – geometrical factor, calculated using a set of equations described in the literature [31].

Present results indicate that the validity of calculations is mostly influenced by strip thickness (h) between two stands because only thickness before first stand and final thickness can be measured.

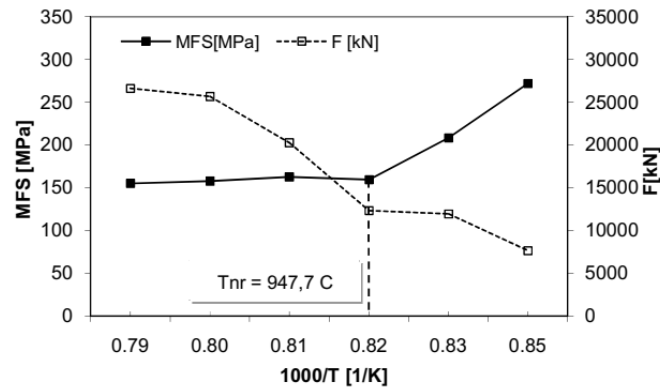


Fig. 11. MFS vs. temperature dependence during rolling one 0.034Nb-0.108C-1.00Mn 4.16 mm thick steel strip [32].

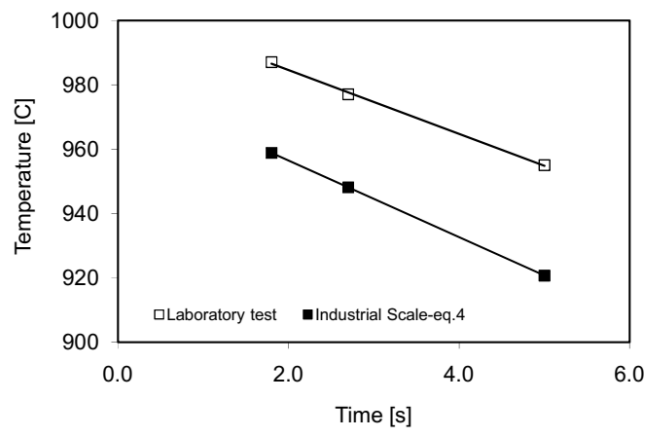


Fig. 12. The influence of interpass time on Tnr (□-laboratory test; ■-industrial scale) for Nb/Ti steel [32].

The T_{nr} temperature of microalloyed steels has been established from rolling mill log data obtained from Hot Strip Mill Smederevo and compared with values obtained from hot-torsion tests in a laboratory simulation. Results obtained in this work show reasonable agreement between T_{nr} temperatures estimated from hot rolling mill data and hot torsion, confirming previously reported behavior [32-37].

Static Recrystallization

Since static recrystallization should be controlled between passes, its kinetics and influences of processing parameters are defined by the Johnson-Mehl-Avrami-Kolmogorov equation (5) [38]:

$$X = 1 - \exp\left[-0.693 \cdot \left(\frac{t}{t_{0.5}}\right)^n\right] \quad 5$$

where: X - recrystallized fraction,

n - Avrami exponent,

t - time, and

$t_{0.5}$ - time for 50% recrystallization, calculated using the following equation:

$$t_{0.5} = A \cdot \varepsilon^p \cdot \dot{\varepsilon}^q \cdot d_0^r \cdot \exp\left(\frac{Q_{SRX}}{R \cdot T}\right) \quad 6$$

where: A , p , q , r , R are constants, ε is strain per pass, $\dot{\varepsilon}$ is strain rate, d_0 is initial grain size, T is temperature, and Q_{SRX} is the activation energy for static recrystallization.

Boratto test [24] was inspired by the industrial practice and designed to determine T_{nr} temperature, as the lowest temperature above which full static recrystallization takes place. Therefore, T_{nr} temperatures are, in all cases, related to an equal amount of recrystallized fraction, enabling plotting $\ln t$ vs. $1/T_{nr}$ dependence [39-41].

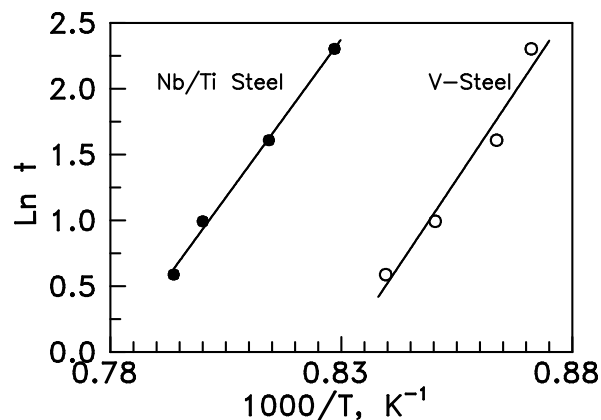


Fig. 13. Time-temperature dependences for Nb and V steel [39, 40].

Since above T_{nr} full static recrystallization takes place, it allowed activation energy for static recrystallization, Q_{SRX} , to be determined; values of 258 kJ/mol for Nb steel and 274 kJ/mol for V-steel were obtained. These values are in good agreement with previously reported results [1]. Below T_{nr} recrystallization is incomplete and/or suppressed, i.e. the mechanism of retardation is not unambiguous and activation energy for static recrystallization, Q_{SRX} , has no apparent physical meaning below T_{nr} [40].

Conclusions

The apparent activation energy for hot working, Q_{HW} , is found to be strain and temperature-dependent, and even interpass time dependant in multipass tests.

The high-temperature Q_{HW}^{Us} , which describe the temperature dependence of the flow stress above the T_{nr} , are close to that of austenite self-diffusion, Q_{SD} , irrespective of either steel composition or test variables.

The low-temperature Q_{HW}^{Ls} , which describe the temperature dependence of the flow stress below the T_{nr} are not only considerably higher but also interpass time-dependent. Interpass time is attributed to suppression of recrystallization (by solute drag or precipitation).

It is concluded that T_{nr} temperature indicates the start of recrystallization suppression, while Q_{HWL} describes the extent of the suppression.

T_{nr} can be estimated on both laboratory and industrial scale. In the case of a very high cooling rate, T_{nr} method is not sensitive, so that T_{rl} and T_{rs} must be calculated via fraction softening.

Multipass Boratto tests also enable the determination of activation energy for static recrystallization, Q_{SRX} , based on T_{nr} temperatures in a fully recrystallized temperature region.

Acknowledgments

This paper is dedicated to prof. Djordje (George) Drobnjak, Professor at Department of Metallurgical Engineering, Faculty of Technology and Metallurgy, University of Belgrade, a leading metallurgist who had introduced a variety of different research topics and modernized teaching activities on Department of Metallurgical Engineering. Work with prof Drobnjak and his mentorship was inspiration and privilege.

References

- [1] T. Gladman, Physical Metallurgy of Microalloyed Steels, IOM London (1997).
- [2] K. Hulka, Niobium Microalloyed High Strength Low Alloy Steels, Metal'96 Int. Conf. Proceedings, Ostrava, Vol. III (1996) 1-10.
- [3] Dj. Drobnjak, Physical Metallurgy (in Serbian), TMF, Beograd (1984).
- [4] W. Mueschenborn, K.P. Imlau, L. Meyer, U. Schrieffer: Recent Developments in Physical Metallurgy and Processing Technology of Microalloyed Flat Rolled Steels, in Microalloying 95, Ed. Korchynsky, ISS, Warrendale (1995) 35-48.
- [5] T. Tanaka, Science and Technology of Hot Rolling of Steel, Ibid, 165-181.
- [6] F. Siciliano, J.J. Jonas: Metallurgical Transactions A, 31A (2000) 511-530.
- [7] Dj. Drobnjak, A. Koprivica, Microalloyed Bar and Forging Steels, Edited by C.J. Van Tyne, G. Krauss, D.K. Matlock, The Minerals, Metals & Materials Society, (1996) 93-107.

- [8] D. Glišić, N. Radović, A. Koprivica, A. Fadel, Dj. Drobnjak, *ISIJ International* 50 (2010) 601-606.
- [9] Yu. Fujita, N. Yurioka: *The Paton Welding Journal*, 558-559 (2000) 139-144.
- [10] N. Radović, Dj. Drobnjak: *Zavarivanje i zavarene konstrukcije*, XLVI (2001) 81.
- [11] N. Yurioka: *Science and Technology of Welding and Joining in the 21th Century and Prospectives toward the 21th Century*, Document IIW IX-1963-2000 (2000) 1-10.
- [12] B. De Meester: *ISIJ International*, 37 (1997) 537-551.
- [13] Garofalo, F.: *Fundamentals of Creep and Creep Rupture in Metals*, Macmillan, New York (1965).
- [14] W. Roberts, *Deformation, Processing and Structure*, ed. by G. Krauss, ASM, Metals Park, (1984) 111.
- [15] J.J. Jonas, C.M.Sellars: *Future Developments of Metals And Ceramics*, ed by J.A. Charles, G.W. Greenwood and G.C. Smith, The Institute of Materials, London, (1992) 147.
- [16] C.M. Sellars, W.J. Mc. Tegart: *Acta Metallurgica*, 14 (1966), 1136.
- [17] Dj. Drobnjak, N. Radovic, M. Andjelic, A. Koprivica: *Steel Research*, 68 (1997) 306.
- [18] Dj. Drobnjak, N. Radović, B. Djurić: *Effect of Test Variables on Q_{HW} and Tnr*, 37th MWSP Conference Proceedings, ISS (1995) 759-769
- [19] N. Radovic, Dj. Drobnjak: *ISIJ International*, 39 (1999) 575.
- [20] Dj. Drobnjak, N. Radovic, *Recrystallization '92*, M.Fuentes and J.Gill Sevilliano, Eds., *Mat. Sci. Forum*, 113-115 (1993) 411-416.
- [21] R. Milovic, D. Manojlovic, M. Andjelic, Dj. Drobnjak: *Steel Research*, 63 (1992) 78-84.
- [22] C. Imbert, M.D. Ryan, H.J. McQueen: *Metallurgical Transactions A*, 15A (1984) 1855-1864.
- [23] M. Sellars, *The Physical Metallurgy of Hot Working*, The Metals Society, London (1980) 3-14.
- [24] F. Boratto, R. Barbosa, S. Yue, J.J. Jonas, *THERMEC-88*, I.Tamura, Ed., *Iron and Steel Institute of Japan*, Tokyo, Japan, Vol.1 (1988) 383-389.
- [25] D.Q. Bai et al., *Processing, Microstructure and Properties of Microalloyed and Other Low Alloy Steels*, ed by A.J.DeArdo, TMS, Warrendale, (1991) 165.
- [26] W.P. Sun et al.: *Recrystallization'92*, ed by M.Fuentes and J. Gill Sevilliano, *Materials Science Forum*, 113-115, (1993) 533.
- [27] D.Q.Bai et al.: *Metallurgical Transactions A*, 24A (1993) 2151.
- [28] B. Dutta, C.M.Sellars: *Materials Science and Technology*, 3 (1987) 197-206.
- [29] W.J. Liu, M.G. Akben: *Canadian Metallurgical Quarterly*, 26 (1987) 145-153.
- [30] R.B. Sims, *Proc. Inst. Mech. Eng.* (1956) 191.
- [31] T. Maccagno et al., *ISIJ International*, 34 (1994) 917-922.
- [32] N. Radović, G. Vukićević, D. Jeremić, Dj. Drobnjak: *Journal of Materials Processing Technology*, 172 (2001) B.9.1-B.9.10.
- [33] N. Radović, G. Vukićević, D. Jeremić, Dj. Drobnjak: *Metalurgija*, 7 (2001) 13-20.
- [34] G. Vukićević, N. Radović, D. Jeremić Dj. Drobnjak: *Metalurgija*, 7 (2001) 151-158.
- [35] N. Radović, G. Vukićević, D. Jeremić, Dj. Drobnjak: *Metalurgija*, 8 (2002) 31-38.
- [36] N. Radović, G. Vukićević, D. Jeremić, Dj. Drobnjak, *Mathematical Modelling of Mechanical Properties of Microalloyed Hot Strip*, *Proceedings of the Int.Conf on Thermomechanical Processing: Mechanics, Microstructure & Control*, Eds.

- E.J.Palmiere, M.Mahfouf and J.Beynon, 23-26 June 2002 Sheffield, University of Sheffield, 413-417.
- [37] S. Vervynckt, K. Verbeken, B. Lopez, and J.J. Jonas, Modern HSLA steels and role of non-recrystallization temperature, *Int. Mater. Rev.*, 57 (2012) 187-207.
- [38] D.A. Porter and K.E. Easterling, Phase Transformations in Metals and Alloys, Van Nostrand Reinhold (UK) Co. Ltd, Wokingham, England (1983)
- [39] N. Radović, Dj. Drobňjak, K. Raić, Determination of Activation Energy for Static Recrystallization using Multipass Continuous Cooling Test, 1st Joint Intl. Conf on Recrystallization and Grain Growth, Eds. G.Gottstein and D.A.Molodov, Aachen, Springer Verlag, Vol. I (2001) 791-796
- [40] N. Radović, Dj. Drobňjak, K. Raić: *Metalurgija*, 15 (2009) 99-104.
- [41] V. Rajinikanth, T. Kumar, B. Mahato, et al.: *Metall and Mat Trans A*, 50A (2019) 5816–5838.



Creative Commons License

This work is licensed under a Creative Commons Attribution 4.0 International License.